



# Cosmological strangeness abundance

Cheng Tao Yang\*, Johann Rafelski

Department of Physics, The University of Arizona, Tucson, AZ 85721, USA

## ARTICLE INFO

### Article history:

Received 25 August 2021

Received in revised form 22 December 2021

Accepted 29 January 2022

Available online 2 February 2022

Editor: P. Brax

## ABSTRACT

We investigate the strange particle composition of the expanding early Universe in the hadron epoch  $T_h \approx 150 \geq T \geq 10$  MeV. We study strangeness yield in thermal and chemical equilibrium constrained by prescribed conserved entropy per baryon in a charge neutral and strangeness neutral ( $s - \bar{s}$ ) Universe. Turning to kinetic processes in a Hubble expanding Universe, we determine the conditions at which at decreasing temperature  $T$  individual strangeness producing reactions fall out of detailed balance between decay and back-reaction strangeness production rates: This is done by comparing the relevant reaction rates to the Hubble expansion rate. We allow for weak, electromagnetic, and strong interaction processes. The weak interaction  $\mu^\pm + \nu_\mu \rightarrow K^\pm$  freezeout is at  $T_f^{K^\pm} = 33.8$  MeV; the electromagnetic process  $l^- + l^+ \rightarrow \phi$  freezeout is at  $T_f^\phi = 23 \sim 25$  MeV; and the hadronic reaction  $\pi + \pi \rightarrow K$  freezeout is at  $T_f^K = 19.8$  MeV.

© 2022 The Author(s). Published by Elsevier B.V. This is an open access article under the CC BY license (<http://creativecommons.org/licenses/by/4.0/>). Funded by SCOAP<sup>3</sup>.

## 1. Introduction

In order to fully describe the nonequilibrium processes in the early Universe we explore here the strangeness abundance and decoupling after normal matter formation in hadronization of quark-gluon plasma (QGP). Nonequilibrium conditions in the early Universe are of general interest: they are understood to be prerequisite for the arrow of time dependent processes to take hold in the Hubble expanding Universe. The two well-studied cases are:

- i) The Big Bang Nucleosynthesis [1–4] (BBN) appears in the temperature range  $0.07 > T > 0.01$  MeV, about 1000 times smaller compared to what will be considered here,  $T_h \approx 150 \geq T \geq 10$  MeV. Certain light isotopes, e.g. Lithium, are residual small remnants of this Universe era;
- ii) Baryogenesis is believed to occur at or before the Universe underwent electroweak (EW) phase transition [2] at a temperature  $T \simeq 130$  GeV, about 1000 times larger compared to the temperature range we consider.

However, the expected EW baryogenesis rate is small and some additional mechanism is required: Heavy bottom flavor decoupling near to the deconfined QGP transformation to the hadron gas (HG) phase just at the upper range of our present consideration may offer alternate baryogenesis opportunity [5].

We begin presenting the equilibrium hadron content of the Universe [6,7], allowing for the presence of strange quark flavor for the given present day entropy per baryon assumed to also govern the hadron era charge neutral and strangeness neutral Universe. We use here standard methods developed in the study of QGP and HG properties created in relativistic heavy ion (RHI) collisions. Ref. [8] provides appropriate introduction.

Moving beyond equilibrium Universe, we generalize the RHI collision strangeness abundance study by Koch, Müller and Rafelski [9] to include electromagnetic and weak interaction processes. We apply methods of kinetic theory seeking the temperature at which strangeness decouples and disappears from the Universe. We illustrate our approach considering an unstable strange particle, say  $S$ , decaying into two particles  $1 + 2$ . In a dense and high temperature plasma with particle 1 and 2 present in thermal equilibrium, the inverse reaction  $1 + 2 \rightarrow S$  produces the particle  $S$ . The natural decay of particles concerned provides also the intrinsic strength of the inverse, strangeness production reaction.

As long as both decay and production reactions are possible, particle  $S$  abundance remains in thermal equilibrium. This balance between production and decay rates is called detailed balance. We used this method before when considering the abundance (non)equilibrium of hadrons driven by reaction  $\pi^0 \leftrightarrow \gamma + \gamma$  [10], and we validate these early results in this work.

Once the primordial Universe expansion rate, given as the inverse of the Hubble parameter  $1/H$ , overwhelms the strongly temperature dependent back-reaction, the decay  $S \rightarrow 1 + 2$  occurs out of balance and particle  $S$  disappears from the inventory. The two-on-two strangeness producing  $S + 3 \leftrightarrow 1 + 2$  reactions have a

\* Corresponding author.

E-mail address: [chengtaoyang@email.arizona.edu](mailto:chengtaoyang@email.arizona.edu) (C.T. Yang).

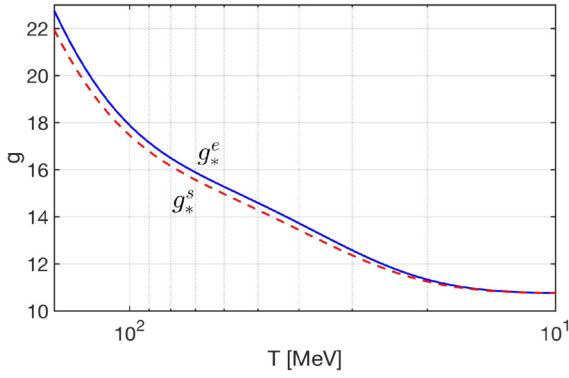


**Fig. 1.** For temperature  $T$  in the early Universe epoch explored in this work  $T_h \approx 150 \geq T \geq 10$  MeV we show the number of effective 'energy' degrees of freedom  $g_*^e$  (solid, blue line), and number of effective 'entropy' degree of freedom  $g_*^s$  (dashed, red line).

significantly higher strangeness production reaction threshold, thus especially near to strangeness decoupling their influence is negligible. Such reactions are more important near the QGP hadronization temperature  $T \simeq 150$  MeV; and they characterize strangeness exchange reactions such as  $K+N \leftrightarrow \Lambda + \pi$ , see Chapter 18 in Ref. [8], which we also explore.

## 2. Hubble expansion

An important assumption allowing us to explore the early Universe evolution is that both baryon and entropy content of the Universe is conserved in the comoving volume, scaling with the third power of the expansion parameter  $a(t)$ , where  $H = \dot{a}/a$ . The authors are not aware of any process capable of altering the baryon number or entropy conservation in significant manner in the evolution period of the hadronic Universe  $T = 150 \sim 10$  MeV. We discuss below the entropy generation, the baryon number is more strictly conserved. Therefore in this study we follow the usual assumption of an adiabatic Universe in which the ratio of baryon number density to visible matter entropy density remains constant during hadronic epoch

$$\frac{n_B - n_{\bar{B}}}{\sigma} = \frac{n_B - n_{\bar{B}}}{\sigma} \Big|_{t_0} = \text{Const.} \quad (1)$$

The subscript  $t_0$  denotes the present day condition, assumed to be the same as in the hadronic era, and  $\sigma$  is the total entropy density (photons, electrons, muons, neutrinos, pions and residual hadrons). In general the entropy density in the early Universe can be written as

$$\sigma = \left( \frac{\rho + P}{T} - \sum_i \frac{\mu_i}{T} n_i \right) = \frac{2\pi^2}{45} g_*^s T^3, \quad (2)$$

where  $g_*^s$  counts the effective number of 'entropy' degrees of freedom. In Fig. 1  $g_*^s$  is shown (dashed, red) as a function of temperature  $T$ . The effect of particle mass threshold [11] is considered in the calculation for all involved particles. When  $T$  decreases below the mass of particle  $T \ll m_i$ , this particle species becomes non-relativistic; the contribution to  $g_*^s$  becomes negligible, creating the dependence on  $T$  seen in Fig. 1.

In the epoch of interest the Universe is dominated by radiation and effectively massless matter behaving like radiation. Therefore the Hubble parameter can be written as [2]

$$H^2 = H_{\text{rad}}^2 \left( 1 + \frac{\rho_{\pi, \mu, \rho}}{\rho_{\text{rad}}} + \frac{\rho_{\text{strange}}}{\rho_{\text{rad}}} \right) = \frac{8\pi^3 G_N}{90} g_*^e T^4, \quad (3)$$

**Table 1**

For a sample of values of temperature  $T$  we show the characteristic Universe time constant  $H^{-1} = \dot{a}/a$ , the age of hadron phase  $t_h$ , and the number  $N$  of e-folds.

$T$ [MeV]	$H^{-1}$ [s]	$t_h$ [s]	$N$ [e-folds]
150	$4.51 \times 10^{-5}$	0	0
100	$1.14 \times 10^{-4}$	$3.45 \times 10^{-5}$	0.46
50	$5.07 \times 10^{-4}$	$2.31 \times 10^{-4}$	1.21
10	$1.49 \times 10^{-2}$	$7.44 \times 10^{-3}$	2.90
5	$5.90 \times 10^{-2}$	$2.95 \times 10^{-2}$	3.59

where:  $g_*^e$  is the total number of effective relativistic 'energy' degrees of freedom seen in Fig. 1 (solid, blue) as a function of temperature  $T$ ;  $H_{\text{rad}}^2 = 8\pi G_N \rho_{\text{rad}}/3$ ;  $G_N$  is the Newtonian constant of gravitation; the 'radiation' energy density includes  $\rho_{\text{rad}} = \rho_\gamma + \rho_\nu + \rho_{e^\pm} = g^e \pi^2 T^4/30$  with  $g^e = 10.75$  for photons, neutrinos, and massless electrons (positrons), see the limit of low  $T$  in Fig. 1. We further note in Eq. (3) a massive-particle correction  $\rho_{\pi, \mu, \rho} = \rho_\pi + \rho_\mu + \rho_\rho$ ; and at highest  $T$  of interest, also of (minor) relevance,  $\rho_{\text{strange}} = \rho_{K^0} + \rho_{K^\pm} + \rho_{K^*} + \rho_\eta + \rho_{\eta'}$  is shown creating the behavior seen for high  $T$  in Fig. 1.

In a kinetic model of neutrino decoupling [12,13] only minor entropy generating processes were observed, the existent entropy redistributes among the various components of the cosmic fluid confirming the strongly adiabatic nature of this decoupling process. The magnitude of entropy increase  $\delta S/S \simeq 3 \times 10^{-5}$  was reported in Ref. [14], see bottom frame in Fig. 9. In the hadronic Universe in the presence of detailed balance (dynamic equilibrium) between different reactions, no entropy can be produced.

However, production of entropy can occur when the expansion of Universe breaks the detailed balance. This occurs for example when a particle can be produced in different reactions and one of the minor but relevant partial rates is smaller compared to the rate of expansion of the Universe  $H$ . Complete decoupling from equilibrium occurs once all production reactions become ineffective in maintaining the dynamical equilibrium, we have the last decay for the unstable particle. A more detailed study of entropy production will be presented in separate work [15].

In the epoch of interest and within the context of the  $\Lambda$ CDM standard model of the Universe, dark energy and massive dark matter contribute negligibly to the energy density: The cold dark matter (CDM) energy content emerges along with visible matter once radiation content decreased from once overwhelming contribution to energy inventory, allowing CDM to become the dominant matter component today. Dark energy is interpreted as the Einstein cosmological parameter  $\Lambda$  emerging in the energy inventory very near to the present time epoch.

In Table 1 we show for a sample of temperature values  $T$  in the 1st column the characteristic Universe expansion time constant  $H^{-1}$  in the 2nd column, the elapsed time  $t_h$  in the Universe after hadronization in the 3rd column, and the number of e-folds  $N$  in the 4th column. To obtain the elapsed time we have set the initial age of the Universe at onset of hadronization to be 45  $\mu$ s; by the time the Universe reaches the next sample point of  $T = 100$  MeV our result is independent of this choice of initial condition. The Universe  $N$ -folding is defined as usual [16]

$$N \equiv \ln \left( \frac{a(t_f)}{a(t_i)} \right) = \int_{t_i}^{t_f} H dt. \quad (4)$$

For a given value  $N$  the Universe scale factor  $a(t)$  has expanded by a factor  $e^N$ . The values of  $N$  we see are near to the values expected for a radiation dominated Universe ( $Ta = \text{Const.}$ ), in which case we

would expect at  $T = 5$  MeV a value  $N = \ln(150/5) = 3.4$ . The deviation  $3.6 > 3.4$  arises during the epoch  $5 < T < 150$  MeV since muons and pions present in very significant abundance at  $T = 150$  MeV disappear from the inventory, reheating the Universe.

We see in Table 1 that the epoch  $10 < T < 150$  MeV of interest to us lasts 7.4 milliseconds, which is in the realm of elementary processes is a much longer time interval than all natural time constants, except the lifespan of the neutron not of relevance in our study. This means that the particle decoupling from the primordial plasma arises because the back-particle formation of a decay process has slowed down at low temperature and is unable to keep up with the speed of Universe expansion.

### 3. Chemical potential and particle abundances

As long as back reactions are faster than the Universe expansion, which condition(s) we characterize in the following, we can explore the Universe composition assuming both kinetic and particle abundance equilibrium (chemical equilibrium). In prior works [6,7] charge neutrality and prescribed conserved baryon-per-entropy-ratio  $(n_B - n_{\bar{B}})/\sigma$  were used to determine the baryochemical potential  $\mu_B$ .

It is convenient to introduce the chemical fugacity for strangeness  $\lambda_s$  and quark  $\lambda_q$  as follows:

$$\lambda_s = \exp(\mu_s/T) \quad \lambda_q = \exp(\mu_B/3T), \quad (5)$$

where  $\mu_s$  and  $\mu_q$  are the chemical potential of strangeness and quark respectively. Imposing  $\langle s - \bar{s} \rangle = 0$ , when the baryon chemical potential does not vanish the chemical potential of strangeness in the early Universe, satisfies (see Section 11.5 in Ref. [8])

$$\lambda_s = \lambda_q \sqrt{\frac{F_K + \lambda_q^{-3} F_Y}{F_K + \lambda_q^3 F_Y}}, \quad (6)$$

where we employ the phase-space function  $F_i$  for sets of nucleon  $N$ , kaon  $K$ , and hyperon  $Y$  particles defined in Ref. [8], Section 11.4.

$$F_N = \sum_{N_i} g_{N_i} W(m_{N_i}/T), \quad N_i = n, p, \Delta(1232), \quad (7)$$

$$F_K = \sum_{K_i} g_{K_i} W(m_{K_i}/T), \quad K_i = K^0, \bar{K}^0, K^\pm, K^*(892), \quad (8)$$

$$F_Y = \sum_{Y_i} g_{Y_i} W(m_{Y_i}/T), \quad Y_i = \Lambda, \Sigma^0, \Sigma^\pm, \Sigma(1385), \quad (9)$$

where  $g_{N_i, K_i, Y_i}$  are the degenerate factors,  $W(x) = x^2 K_2^B(x)$  with  $K_2^B$  is the modified Bessel function of integer order "2". Considering the Boltzmann approximation for the particle number density we have

$$n_N = \frac{T^3}{2\pi^2} (\lambda_q^3 - \lambda_q^{-3}) F_N, \quad (10)$$

$$n_K = \frac{T^3}{2\pi^2} (\lambda_s \lambda_q^{-1} - \lambda_s^{-1} \lambda_q) F_K, \quad (11)$$

$$n_Y = \frac{T^3}{2\pi^2} (\lambda_q^2 \lambda_s - \lambda_q^{-2} \lambda_s^{-1}) F_Y. \quad (12)$$

Then the net baryon density in early Universe with temperature range  $10 < T < 150$  MeV can be written as

$$\begin{aligned} & \frac{(n_B - n_{\bar{B}})}{\sigma} \\ &= \frac{1}{\sigma} [(n_p - n_{\bar{p}}) + (n_n - n_{\bar{n}}) + (n_Y - n_{\bar{Y}})] \end{aligned}$$

$$\begin{aligned} &= \frac{T^3}{2\pi^2 \sigma} \left[ (\lambda_q^3 - \lambda_q^{-3}) F_N + (\lambda_q^2 \lambda_s - \lambda_q^{-2} \lambda_s^{-1}) F_Y \right] \\ &= \frac{T^3}{2\pi^2 \sigma} (\lambda_q^3 - \lambda_q^{-3}) F_N \left[ 1 + \frac{\lambda_s}{\lambda_q} \left( \frac{\lambda_q^3 - \lambda_q^{-1} \lambda_s^{-2}}{\lambda_q^3 - \lambda_q^{-3}} \right) \frac{F_Y}{F_N} \right] \\ &\approx \frac{T^3}{2\pi^2 \sigma} (\lambda_q^3 - \lambda_q^{-3}) F_N \left[ 1 + \frac{\lambda_s}{\lambda_q} \frac{F_Y}{F_N} \right], \quad (13) \end{aligned}$$

where we can neglect the term  $F_Y/F_N$  in the expansion of Eq. (6) in our  $T$ -range.

Introducing strangeness  $\langle s - \bar{s} \rangle = 0$  constraint and using the entropy density Eq. (2), the explicit relation for baryon to entropy ratio becomes

$$\begin{aligned} \frac{n_B - n_{\bar{B}}}{\sigma} &= \frac{45}{2\pi^4 g_*^3} \sinh \left[ \frac{\mu_B}{T} \right] F_N \\ &\times \left[ 1 + \frac{F_Y}{F_N} \sqrt{\frac{1 + e^{-\mu_B/T} F_Y/F_K}{1 + e^{\mu_B/T} F_Y/F_K}} \right]. \quad (14) \end{aligned}$$

Governing Eq. (14) is the present-day baryon-per-entropy-ratio, and we obtain the value

$$\frac{n_B - n_{\bar{B}}}{\sigma} \Big|_{t_0} = (0.865 \pm 0.008) \times 10^{-10}. \quad (15)$$

The value we obtained in Eq. (15) is 12% larger compared to the year 2003 Ref. [6] where  $0.77 \pm 0.06 \times 10^{-10}$  was used; this difference is due to a change in input parameters describing properties of the Universe. For a detailed evaluation method we refer to this earlier work now using a baryon-to-photon ratio [16]:  $(n_B - n_{\bar{B}})/n_\gamma = (0.609 \pm 0.06) \times 10^{-9}$ , as well as the entropy per particle for a massless boson  $\sigma/n|_{\text{boson}} \approx 3.60$  and massless fermion  $\sigma/n|_{\text{fermion}} \approx 4.20$ .

Neutrinos, after decoupling, become a free-streaming cosmic component and follow the Einstein-Vlasov Equation in FRW spacetime governed by the corresponding free-streaming distribution [17]: the free-streaming neutrinos are out of the thermal equilibrium and the conventional relation between entropy, energy density, and pressure does not apply. However, since neutrino decoupling occurs at  $T_k \gg m_\nu$ , the entropy content of free-streaming neutrinos is computed as if neutrinos were massless [17], even when  $T_\gamma < m_\nu$ . Despite the fact that neutrinos decouple near  $T = 2$  MeV, below the here considered temperature range, the above discussion is relevant since we need to connect present day conditions to the hadronic era. Specifically, in the evaluation of baryon-per-entropy-ratio we allow for the reheating of photons by  $e^+e^-$  annihilation, thus the entropy content of photons incorporates that of the  $e^+e^-$  primordial plasma.

We solve Eqs. (6), (14) numerically to obtain Fig. 2 as a function of  $T$ . Our results agree with Ref. [6], allowing for a slightly different set of cosmological parameters, as noted above. The chemical potentials change dramatically in the temperature window  $50 \leq T \leq 30$  MeV, which behavior is describing the process of antibaryon disappearance. Substituting the chemical potential  $\lambda_q$  and  $\lambda_s$  into Eq. (10), (11), (12) we can obtain the particle number densities for different species. In Fig. 3 we show examples of particle abundance ratios. Of special interest is the temperature where antibaryons disappear from the Universe inventory, defined when the ratio  $n_{\bar{B}}/(n_B - n_{\bar{B}}) = 1$ . This condition is reached in an expanding Universe at  $T = 38.2$  MeV. Considering  $n_Y/n_B$  we see that hyperons  $Y(sq\bar{q})$  remain a noticeable 1% component in baryon yield through this domain of antibaryon decoupling.

Pions  $\pi(q\bar{q})$  are the most abundant hadrons because of their low mass and the reaction  $\gamma\gamma \rightarrow \pi^0$ , which assures chemical yield equilibrium [10]; see brown line for  $n_\pi/n_B \gg 1$  in Fig. 3. We can understand some of counterintuitive results appearing at

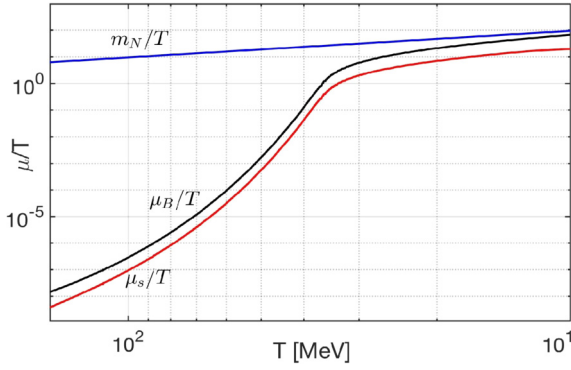


**Fig. 2.** The chemical potential of baryon  $\mu_B/T$  and strangeness  $\mu_s/T$  as a function of temperature  $150 \text{ MeV} > T > 10 \text{ MeV}$  in the early Universe; for comparison we show  $m_N/T$  with  $m_N = 938.92 \text{ MeV}$ , the average nucleon mass.

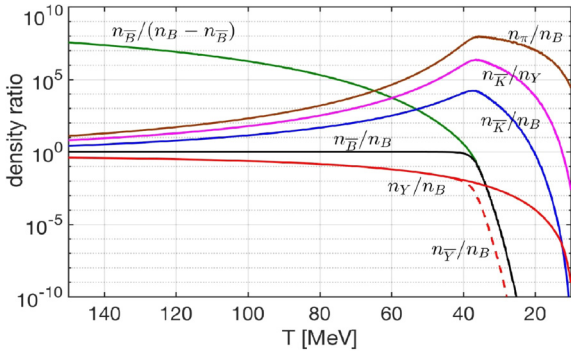


**Fig. 3.** Ratios of hadronic particle number densities as a function of temperature  $150 \text{ MeV} > T > 10 \text{ MeV}$  in the early Universe with baryon  $B$  yields: pions  $\pi$  (brown line), kaons  $K(q\bar{s})$  (blue), antibaryon  $\bar{B}$  (black), hyperon  $Y$  (red) and anti-hyperons  $\bar{Y}$  (dashed red). Also shown  $\bar{K}/Y$  (purple).

low temperatures by remembering that the threshold energy for strangeness in  $\Lambda(uds)$  costs less energy compared to  $K(q\bar{s})$ : For  $150 \text{ MeV} > T > 20 \text{ MeV}$  we see the ratio  $n_{\bar{K}(q\bar{s})}/n_B \gg 1$  which implies pair abundance of strangeness is more abundant than baryons, and is dominantly present in mesons, since  $n_{\bar{K}}/n_Y \gg 1$ ; for  $12.9 \text{ MeV} > T$  we have  $n_Y/n_B > n_{\bar{K}}/n_B$ , now the still existent tiny abundance of strangeness is found predominantly in hyperons. We find below that the exchange reaction  $\bar{K} + N \rightarrow \Lambda + \pi$  can re-equilibrate kaons and hyperons in the temperature range; therefore strangeness symmetry  $s = \bar{s}$  is maintained.

#### 4. Strangeness abundance decoupling

The reaction rates for inelastic collision process capable of changing particle number, for example  $\pi\pi \rightarrow K^0$ , is suppressed by the factor  $\exp(-m_{K^0}/T)$ . On the other hand, there is no suppression for the elastic momentum and energy exchanging particle collisions in plasma. We conclude that for the case  $m \gg T$ , the dominant collision term in the relativistic Boltzmann equation is the elastic collision term keeping all heavy particles in kinetic energy equilibrium with the plasma. This allows to study the particle abundance in plasma presuming the energy-momentum statistical distribution equilibrium exists. This insight was in detail discussed in the preparator phase of laboratory exploration of hot hadron and quark matter, see Ref. [9].

In order to study the particle abundance in the Universe when  $m \gg T$ , instead of solving the exact Boltzmann equation, we can separate the fast energy-momentum equilibrating collisions from the slow particle number changing inelastic collisions. In the following we explore alone the rates of inelastic collision and com-

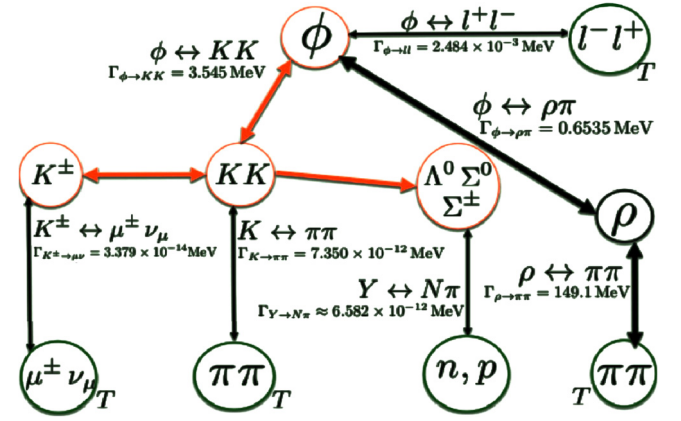


**Fig. 4.** The strangeness abundance changing reactions in the primordial Universe. The red circles show strangeness carrying hadronic particles; red thick lines denote effectively instantaneous reactions. Black thick lines show relatively strong hadronic reactions. The reaction rates required to describe strangeness time evolution are shown in Ref. [20].

pare the relaxation times of particle production in all relevant reactions, one with another and with the Universe expansion rate.

In order to determine where exactly strangeness disappears from the Universe inventory we explore the magnitudes of a relatively large number of different rates of production and decay processes, and compare these with the Hubble time constant. The reactions at some point relevant to strangeness evolution in the considered Universe evolution epoch  $T_h \approx 150 \geq T \geq 10 \text{ MeV}$  are illustrated in Fig. 4 and the pertinent reaction strength is indicated. As shown:

- We study strange quark abundance in baryons and mesons, considering both open and hidden strangeness (hidden:  $s\bar{s}$ -content). Important source reactions are  $l^- + l^+ \rightarrow \phi$ ,  $\rho + \pi \rightarrow \phi$ ,  $\pi + \pi \rightarrow K_S$ ,  $\Lambda \leftrightarrow \pi + N$ , and  $\mu^\pm + \nu \rightarrow K^\pm$ .
- Muons and pions are coupled through electromagnetic reactions  $\mu^+ + \mu^- \leftrightarrow \gamma + \gamma$  and  $\pi \leftrightarrow \gamma + \gamma$  to the photon background and retain their chemical equilibrium until the temperature  $T = 4 \text{ MeV}$  and  $T = 5 \text{ MeV}$ , respectively [18,10]. The large  $\phi \leftrightarrow K + K$  rate assures  $\phi$  and  $K$  are in relative chemical equilibrium.

##### 4.1. Strangeness in meson era

The thermal reaction rate per time and volume for two body-to-one particle reactions  $1 + 2 \rightarrow 3$  has been presented before [9, 10,19]. In full kinetic and chemical equilibrium, the reaction rate per time per volume is given by [19]:

$$R_{12 \rightarrow 3} = \frac{g_3}{(2\pi)^2} \frac{m_3}{\tau_3^0} \int_0^\infty \frac{p_3^2 dp_3}{E_3} \frac{e^{E_3/T}}{e^{E_3/T} \pm 1} \Phi(p_3), \quad (16)$$

where  $\tau_3^0$  is the vacuum lifetime of particle 3. The positive sign “+” is for the case when particle 3 is a boson, and negative sign “-” for fermion. The function  $\Phi(p_3)$  for the non-relativistic limit  $m_3 \gg p_3$ ,  $T$  can be written as

$$\Phi(p_3 \rightarrow 0) = 2 \frac{1}{(e^{E_1/T} \pm 1)(e^{E_2/T} \pm 1)}. \quad (17)$$

Considering the Boltzmann limit, the thermal reaction rate per unit time and volume becomes

$$R_{12 \rightarrow 3} = \frac{g_3}{2\pi^2} \left( \frac{T^3}{\tau_3^0} \right) \left( \frac{m_3}{T} \right)^2 K_1^B(m_3/T), \quad (18)$$

where  $K_1^B$  is the modified Bessel functions of integer order "1". In order to compare the reaction time with Hubble time  $1/H$ , it is convenient to define the relaxation time for the process  $1 + 2 \rightarrow 3$  as follows

$$\tau_{12 \rightarrow 3} \equiv \frac{n_1^{eq}}{R_{12 \rightarrow n}}, \quad n_1^{eq} = \frac{g_1}{2\pi^2} \int_{m_1}^{\infty} dE \frac{E \sqrt{E^2 - m_1^2}}{\exp(E/T) \pm 1}, \quad (19)$$

where  $n_1^{eq}$  is the thermal equilibrium number density of particle 1 with the 'heavy' mass  $m_1 > T$ . Combining Eq. (18) with Eq. (19) we obtain

$$\frac{\tau_{12 \rightarrow 3}}{\tau_3^0} = \frac{2\pi^2 n_1^{eq} T^3}{g_3 (m_3/T)^2 K_1^B(m_3/T)}, \quad n_1^{eq} \simeq g_1 \left(\frac{m_1 T}{2\pi}\right)^{3/2} e^{-m_1/T} \quad (20)$$

where, conveniently, the relaxation time does not depend on the abundant and often relativistic heat bath component 2, e.g.  $l^\pm, \pi, \nu, \gamma$ . The density of heavy particles 1 and 3 can in general be well approximated using the leading and usually nonrelativistic Boltzmann term as shown above.

It is common to refer to particle freeze-out as the epoch where a given type of particle ceases to interact with other particles. In an expanding Universe this can happen when the density of particles becomes too low because of the Universe expansion and the probability for two-particles collision is negligible, or when the particle energy becomes too small to overcome reaction threshold. In this situation the particle yield decouples from the cosmic plasma, a chemical nonequilibrium and even complete abundance disappearance of this particle follow; the condition for the given reaction  $1 + 2 \rightarrow 3$  to decouple is

$$\tau_{12 \rightarrow 3}(T_f) = 1/H(T_f). \quad (21)$$

When presenting the reaction rates and quoting decoupling as a function of temperature  $T$  we must remember that for a temperature range  $50 > T > 5$  MeV, we have  $10^{-1} < dT/dt < 10^{-4}$  MeV/ $\mu$ s. We estimate the width of decoupling (freeze-out) temperature interval  $\Delta T_f$  as follows

$$\frac{1}{\Delta T_f} \equiv \left[ \frac{1}{(\Gamma_{12 \rightarrow 3}/H)} \frac{d(\Gamma_{12 \rightarrow 3}/H)}{dT} \right]_{T_f}, \quad \Gamma_{12 \rightarrow 3} \equiv \frac{1}{\tau_{12 \rightarrow 3}} \quad (22)$$

Using Eq. (3) and Eq. (20) and considering the temperature range  $50 > T > 5$  MeV with  $g_*^e \approx \text{constant}$  we obtain using the Boltzmann approximation to describe the massive particles 1 and 3

$$\frac{\Delta T_f}{T_f} \approx \frac{T_f}{m_3 - m_1 - 2T_f}, \quad m_3 - m_1 \gg T_f. \quad (23)$$

The width of freezeout is shown in right column in Table 2. We see a range of 2-10%. Therefore it is justified to consider as decoupling condition in time the value of temperature at which the pertinent rate cross the Hubble expansion rate, see Fig. 5.

The relevant interaction rates competing with Hubble time involving strongly interacting mesons are the reactions  $\pi + \pi \leftrightarrow K$ ,  $\mu^\pm + \nu \rightarrow K^\pm$ ,  $l^+ + l^- \rightarrow \phi$ ,  $\rho + \pi \leftrightarrow \phi$ , and  $\pi + \pi \leftrightarrow \rho$ . These rates are compared with Hubble time in Fig. 5.

We see that the weak interaction (WI) reaction  $\mu^\pm + \nu_\mu \rightarrow K^\pm$  becomes slower compared to the Universe expansion near temperature  $T_f^{K^\pm} = 33.8$  MeV signaling the onset of abundance nonequilibrium for  $K^\pm$ . For  $T < T_f^{K^\pm}$ , the reactions  $\mu^\pm + \nu_\mu \rightarrow K^\pm$  decouples from the cosmic plasma; the corresponding detailed balance can be broken and the decay reactions  $K^\pm \rightarrow \mu^\pm + \nu_\mu$  are acting like a (small) "hole" in the strangeness abundance "pot". If

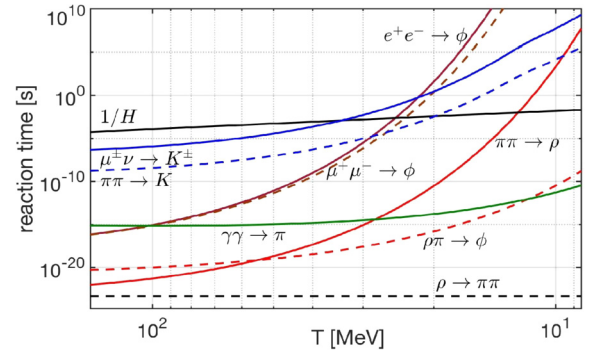


**Fig. 5.** Hadronic relaxation reaction times, see Eq. (19), as a function of temperature  $T$ , are compared to Hubble time  $1/H$  (black solid line). At bottom the horizontal black-dashed line is the natural (vacuum) lifespan of  $\rho$ .

**Table 2**

The characteristic strangeness reaction and their freezeout temperature and temperature width in early Universe.

Reactions	Freezeout Temperature (MeV)	$\Delta T_f$ (MeV)
$\mu^\pm \nu \rightarrow K^\pm$	$T_f = 33.8$ MeV	3.5 MeV
$e^+ e^- \rightarrow \phi$	$T_f = 24.9$ MeV	0.6 MeV
$\mu^+ \mu^- \rightarrow \phi$	$T_f = 23.5$ MeV	0.6 MeV
$\pi \pi \rightarrow K$	$T_f = 19.8$ MeV	1.2 MeV
$\pi \pi \rightarrow \rho$	$T_f = 12.3$ MeV	0.2 MeV

other strangeness production reactions did not exist, strangeness would disappear as the Universe cools below  $T_f^{K^\pm}$ . However, we have other reactions:  $l^+ + l^- \leftrightarrow \phi$ ,  $\pi + \pi \leftrightarrow K$ , and  $\rho + \pi \leftrightarrow \phi$  can still produce the strangeness in cosmic plasma and the rate is very large compared to the WI small decay hole.

In Table 2 we show the characteristic strangeness reactions and their freezeout temperatures in the early Universe. The intersection of strangeness reaction times with  $1/H$  occurs for  $l^- + l^+ \rightarrow \phi$  at  $T_f^\phi = 25 \sim 23$  MeV, and for  $\pi + \pi \rightarrow K$  at  $T_f^K = 19.8$  MeV, for  $\pi + \pi \rightarrow \rho$  at  $T_f^\rho = 12.3$  MeV. The reactions  $\gamma + \gamma \rightarrow \pi$  and  $\rho + \pi \leftrightarrow \phi$  are faster compared to  $1/H$ . However, the  $\rho \rightarrow \pi + \pi$  lifetime (black dashed line in Fig. 5) is smaller than the reaction  $\rho + \pi \leftrightarrow \phi$ ; in this case, most of  $\rho$ -meson decays faster, thus are absent and cannot contribute to the strangeness creation in the meson sector. Below the temperature  $T < 20$  MeV, all the detail balances in the strange meson reactions are broken and the strangeness in the meson sector should disappear rapidly, were it not for the small number of baryons present in the Universe.

#### 4.2. Strangeness in hyperons

We now consider the strangeness production reaction  $\pi + N \rightarrow K + \Lambda$ , the strangeness exchange reaction  $\bar{K} + N \rightarrow \Lambda + \pi$ ; and the strangeness decay  $\Lambda \rightarrow N + \pi$  allowing strange hyperons and anti hyperons to influence the dynamic nonequilibrium condition including development of  $\langle s - \bar{s} \rangle \neq 0$ . The cross sections  $\sigma_{\bar{K}N \rightarrow \Lambda \pi}$  and  $\sigma_{\pi N \rightarrow K \Lambda}$  are obtained from experiment.

The thermal averaged cross sections for the strangeness production and exchange processes are about  $\sigma_{\pi N \rightarrow K \Lambda} \sim 0.1$  mb and  $\sigma_{\bar{K}N \rightarrow \Lambda \pi} = 1 \sim 3$  mb in the energy range we are interested [9]. In addition we use:

1) For the cross section  $\sigma_{\bar{K}N \rightarrow \Lambda \pi}$  we use [9]

$$\sigma_{\bar{K}N \rightarrow \Lambda \pi} = \frac{1}{2} (\sigma_{K-p \rightarrow \Lambda \pi^0} + \sigma_{K-n \rightarrow \Lambda \pi^-}). \quad (24)$$

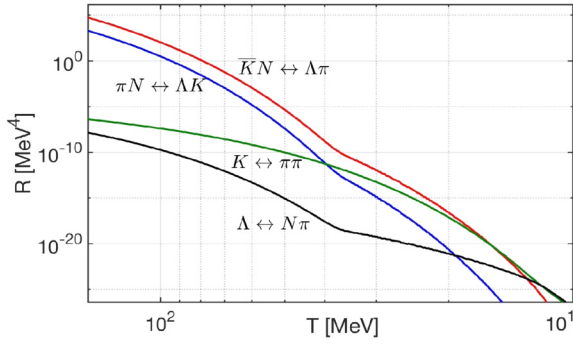


**Fig. 6.** Thermal reaction rate  $R$  per volume and time for important hadronic strangeness production and exchange processes as a function of temperature  $150 \text{ MeV} > T > 10 \text{ MeV}$  in the early Universe.

Here the experimental cross sections can be parameterized as

$$\begin{aligned} \sigma_{K^- p \rightarrow \Lambda \pi^0} &= \begin{cases} 1479.53 \text{ mb} \cdot \exp\left(\frac{-3.377\sqrt{s}}{\text{GeV}}\right), & \text{for } \sqrt{s_m} < \sqrt{s} < 3.2 \text{ GeV} \\ 0.3 \text{ mb} \cdot \exp\left(\frac{-0.72\sqrt{s}}{\text{GeV}}\right), & \text{for } \sqrt{s} > 3.2 \text{ GeV} \end{cases} \end{aligned} \quad (25)$$

$$\begin{aligned} \sigma_{K^- n \rightarrow \Lambda \pi^-} &= 1132.27 \text{ mb} \cdot \exp\left(\frac{-3.063\sqrt{s}}{\text{GeV}}\right), \\ &\text{for } \sqrt{s} > 1.699 \text{ GeV} \end{aligned} \quad (26)$$

where  $\sqrt{s_m} = 1.473 \text{ GeV}$ .

2) For the cross section  $\sigma_{\pi N \rightarrow K \Lambda}$  we use [21]

$$\sigma_{\pi N \rightarrow K \Lambda} = \frac{1}{4} \times \sigma_{\pi p \rightarrow K^0 \Lambda}. \quad (27)$$

The experimental  $\sigma_{\pi p \rightarrow K^0 \Lambda}$  can be approximated as follows

$$\sigma_{\pi p \rightarrow K^0 \Lambda} = \begin{cases} \frac{0.9 \text{ mb} \cdot (\sqrt{s} - \sqrt{s_0})}{0.091 \text{ GeV}}, & \text{for } \sqrt{s_0} < \sqrt{s} < 1.7 \text{ GeV} \\ \frac{90 \text{ MeV} \cdot \text{mb}}{\sqrt{s} - 1.6 \text{ GeV}}, & \text{for } \sqrt{s} > 1.7 \text{ GeV} \end{cases} \quad (28)$$

with  $\sqrt{s_0} = m_\Lambda + m_K$ .

The general form for thermal reaction rate per volume is discussed in [8] (Eq. (17.16), Chapter 17). Given the cross sections, we obtain the thermal reaction rate per volume for strangeness exchange reaction seen in Fig. 6. We see that around  $T = 20 \text{ MeV}$ , the dominant reactions for the hyperon  $\Lambda$  production is  $\bar{K} + N \leftrightarrow \Lambda + \pi$ . At the same time, the  $\pi + \pi \rightarrow K$  reaction becomes slower than Hubble time and kaon  $K$  decay rapidly in the early Universe. However, the anti-kaons  $\bar{K}$  become the hyperon  $\Lambda$  because the strangeness exchange reaction  $\bar{K} + N \rightarrow \Lambda + \pi$  in the baryon-dominated Universe. We have strangeness in  $\Lambda$  and it disappears from the Universe via the decay  $\Lambda \rightarrow N + \pi$ . Both strangeness and anti-strangeness disappear because of the  $K \rightarrow \pi + \pi$  and  $\Lambda \rightarrow N + \pi$ , while the strangeness abundance  $s = \bar{s}$  in the early Universe remains.

Around  $T = 12.9 \text{ MeV}$  the reaction  $\Lambda + \pi \rightarrow \bar{K} + N$  becomes slower than the strangeness decay  $\Lambda \leftrightarrow N + \pi$ , which shows that at the low temperature the  $\Lambda$  particles are still in equilibrium via the reaction  $\Lambda \leftrightarrow N + \pi$  and little strangeness remains in the  $\Lambda$ . Then strangeness abundance becomes asymmetric  $s \gg \bar{s}$ , which shows that the assumption for strangeness conservation can only be valid until the temperature  $T \sim 13 \text{ MeV}$ . Below this temperature a new regime opens up in which the tiny residual strangeness abundance is governed by weak decays with no re-equilibration with mesons. Also, in view of baryon asymmetry,  $\langle s - \bar{s} \rangle \neq 0$ .

## 5. Discussion

We have presented results characterizing the evolution of cosmological strangeness abundance. Our work refines the understanding of the physical phenomena connecting the QGP phase with the neutrino decoupling stage [6,7]. The cosmic neutrino abundance [13] and free-streaming neutrino momentum distribution [17] could influence the speed of Universe expansion [22], a topic generating a lot of interest today [23,24]. Our work contributes insights about the connection between the QGP era and the neutrino decoupling era.

In the QGP epoch before hadronization at temperature  $T > 150 \text{ MeV}$ , the strangeness formation processes explored in the laboratory [8] are fast enough to assure chemical equilibrium. In the phase transformation to hadrons the excess QGP entropy as compared to HG is absorbed in additional Universe comoving volume expansion, while excess strangeness has time to reequilibrate into equilibrium HG abundance, the governing time scales were introduced in Table 1. This situation is opposite to what one encounters in the fast and explosive disintegration of QGP drop created in RHI collisions in the laboratory. The Universe is undergoing a relatively slow on hadronic time scale phase transformation emerging from QGP near to chemical equilibrium abundance of all particles here considered. Tracking the following particle abundance we adopted ratio of baryon to entropy content of the Universe surrounding us today.

Before turning to non-equilibrium processes we have evaluated the chemical equilibrium composition in the following Universe expansion and found several Universe epochs of interest:

- In the temperature range  $20 < T < 60 \text{ MeV}$  the Universe is rich in physics phenomena involving strange mesons, (anti)baryons including (anti)hyperon abundances. Considering the inventory of the Universe strange mesons and baryons, we have reevaluated the temperature of the baryon disappearance, which is estimated qualitatively in Ref. [2] to be  $T = 40\text{-}50 \text{ MeV}$ . We have seen in Fig. 3 (black line) that antibaryons (sum of non-strange and strange anti-hyperons) effectively disappear just below  $T = 40 \text{ MeV}$ .
- We have established in Fig. 3 the regimes in which strangeness is predominantly in mesons or in baryons. We found that for temperature  $150 \text{ MeV} > T > 20 \text{ MeV}$  the Universe is meson-dominant and the strangeness is dominantly present in the meson sector with  $s = \bar{s}$ . For temperature  $T < 20 \text{ MeV}$ , the Universe becomes baryon-dominant. Below temperature  $T < 13 \text{ MeV}$ , strangeness is present dominantly in hyperons, hence  $s - \bar{s} \neq 0$ .

When  $m \gg T$ , instead of solving the exact Boltzmann equation we can separate the fast energy-momentum equilibrating collisions from the slow particle number changing inelastic collisions. We have evaluated inelastic reaction rates involving (strange) mesons and baryons in detail and compare these rates with Hubble expansion rate to find Universe epochs of interest that follow the strength of weak, electromagnetic and strong interactions:

- The first reaction to become slower compared to Hubble time  $1/H$  is the weak interaction  $\mu^\pm + \nu_\mu \rightarrow K^\pm$  at  $T_f^{K^\pm} = 33.8 \text{ MeV}$ .
- This is followed by the electromagnetic process  $l^- + l^+ \rightarrow \phi$  at  $T_f^\phi = 23 \sim 25 \text{ MeV}$ .
- At  $T_f^K = 19.8 \text{ MeV}$  the hadronic reaction  $\pi + \pi \rightarrow K$  becomes slower than the Hubble expansion. In this case, the strangeness in mesons would disappear for  $T < 20 \text{ MeV}$ .

In order to understand strangeness in hyperons, we evaluated the reaction  $\pi + N \rightarrow K + \Lambda$ , the strangeness exchange reaction  $\bar{K} + N \rightarrow \Lambda + \pi$ , and the strangeness decay  $\Lambda \rightarrow N + \pi$ , in detail. In Fig. 6 we saw that for  $T < 20$  MeV, the reactions for the hyperon  $\Lambda$  production are dominated by  $\bar{K} + N \leftrightarrow \Lambda + \pi$ . Both strangeness and anti-strangeness disappear from the Universe via the reactions  $\Lambda \rightarrow N + \pi$  and  $K \rightarrow \pi + \pi$ , keeping the  $s = \bar{s}$ . Beginning with  $T = 12.9$  MeV, the dominant reaction is  $\Lambda \leftrightarrow N + \pi$ , which shows that at a lower temperature we still have (very little) strangeness remnant in the  $\Lambda$ . In this case, the strangeness abundance becomes asymmetric and we have  $s \gg \bar{s}$  in the early Universe. Hence, strange hyperons and anti hyperons could enter into dynamic nonequilibrium condition including  $(s - \bar{s}) \neq 0$ .

Our results depend on the baryon-per-entropy ratio  $(n_B - n_{\bar{B}})/\sigma$  assumed to be constant during Universe evolution. The assumption of co-moving baryon number conservation for  $T < 150$  MeV is justified by the wealth of particle physics experiments. The co-moving entropy conservation presumes (nearly) adiabatically evolving Universe, a common assumption.

However, this situation should be reexamined as we noted above: Even in nearly adiabatically expanding Universe the inverse of a multi-particle decay process of hadrons decouples earlier than the dominant two-to-one reactions we considered here. In this case, multiparticle decays add to entropy inventory while ‘mother’ populations are kept in equilibrium by two-to-one reactions. To describe this novel situation kinetic theory for entropy production needs to be adapted, a topic we hope to address soon [15]. We note that this mechanism was proposed as the origin of electron, positron decoupling in dense medium and source of chemical nonequilibrium in QED plasma [25,26]. Should  $(n_B - n_{\bar{B}})/\sigma$  in hadron epoch be different from the here used present day value, the chemical potential change according to Eq. (14).

The primary conclusion of this first study of strangeness production and content in the early Universe, following on QGP hadronization, is that the relevant temperature domains indicate a complex interplay between baryon and meson (strange and non-strange) abundances and non-trivial decoupling from equilibrium for strange and non-strange mesons. We believe that this work contributes to the opening of a new and rich domain in the study of the Universe evolution in the future. This work is prerequisite for deeper understanding of heavier flavors, for bottom see [5]; we plan to return to the case of charm flavor soon.

### Declaration of competing interest

The authors declare that they have no known competing financial interests or personal relationships that could have appeared to influence the work reported in this paper.

### Acknowledgement

The research of CTY was in part supported by the US Department of Energy under Grant Contract DESC0012704 to the Brookhaven National Laboratory.

### References

- [1] C. Pitrou, A. Coc, J.P. Uzan, E. Vangioni, Precision big bang nucleosynthesis with improved Helium-4 predictions, *Phys. Rep.* 754 (2018) 1–66, <https://doi.org/10.1016/j.physrep.2018.04.005>, arXiv:1801.08023 [astro-ph.CO].
- [2] E.W. Kolb, M.S. Turner, *The early universe*, *Front. Phys.* 69 (1) (1990), 547 pp., ISBN: 0201626748, 9780201626742.
- [3] S. Dodelson, *Modern Cosmology*, Academic Press, Amsterdam, ISBN 9780122191411, 2003, 440 pp.
- [4] V. Mukhanov, *Physical Foundations of Cosmology*, Cambridge University Press, Cambridge, 2005, 441 pp., ISBN: 0521563984, 9780521563987.
- [5] C.T. Yang, J. Rafelski, Possibility of bottom-catalyzed matter genesis near to primordial QGP hadronization, arXiv:2004.06771 [hep-ph].
- [6] M.J. Fromerth, I. Kuznetsova, L. Labun, J. Letessier, J. Rafelski, From quark-gluon universe to neutrino decoupling:  $200 < T < 2$  MeV, *Acta Phys. Pol. B* 43 (12) (2012) 2261–2284, <https://doi.org/10.5506/APhysPolB.43.2261>, arXiv:1211.4297 [nucl-th].
- [7] J. Rafelski, J. Birrell, Traveling through the universe: back in time to the quark-gluon plasma era, *J. Phys. Conf. Ser.* 509 (2014) 012014, <https://doi.org/10.1088/1742-6596/509/1/012014>, arXiv:1311.0075 [nucl-th].
- [8] J. Letessier, J. Rafelski, Hadrons and quark-gluon plasma, *Camb. Monogr. Part. Phys. Nucl. Phys. Cosmol.* 18 (2002), <https://doi.org/10.1017/CBO9780511534997>, 397 pp., ISBN: 9780521018234 (Paperback), 9780521385367 (Hardback), 9780511037276 (Online).
- [9] P. Koch, B. Muller, J. Rafelski, Strangeness in relativistic heavy ion collisions, *Phys. Rep.* 142 (1986) 167–262, [https://doi.org/10.1016/0370-1573\(86\)90096-7](https://doi.org/10.1016/0370-1573(86)90096-7).
- [10] I. Kuznetsova, D. Habs, J. Rafelski, Pion and muon production in e-, e+, gamma plasma, *Phys. Rev. D* 78 (2008) 014027, <https://doi.org/10.1103/PhysRevD.78.014027>, arXiv:0803.1588 [hep-ph].
- [11] A. Coc, K.A. Olive, J.P. Uzan, E. Vangioni, Big bang nucleosynthesis constraints on scalar-tensor theories of gravity, *Phys. Rev. D* 73 (2006) 083525, <https://doi.org/10.1103/PhysRevD.73.083525>, arXiv:astro-ph/0601299 [astro-ph].
- [12] J. Birrell, J. Wilkening, J. Rafelski, Boltzmann equation solver adapted to emergent chemical non-equilibrium, *J. Comput. Phys.* 281 (2015) 896–916, <https://doi.org/10.1016/j.jcp.2014.10.056>, arXiv:1403.2019 [math.NA].
- [13] J. Birrell, C.T. Yang, J. Rafelski, Relic neutrino freeze-out: dependence on natural constants, *Nucl. Phys. B* 890 (2014) 481–517, <https://doi.org/10.1016/j.nuclphysb.2014.11.020>, arXiv:1406.1759 [nucl-th].
- [14] E. Grohs, G.M. Fuller, C.T. Kishimoto, M.W. Paris, A. Vlasenko, Neutrino energy transport in weak decoupling and big bang nucleosynthesis, *Phys. Rev. D* 93 (8) (2016) 083522, <https://doi.org/10.1103/PhysRevD.93.083522>, arXiv:1512.02205 [astro-ph.CO].
- [15] C.T. Yang, J. Rafelski, Entropy production in primordial Universe from  $130 \text{ GeV} > T > 10 \text{ keV}$ , in press.
- [16] M. Tanabashi, et al., Particle Data Group, Review of particle physics, *Phys. Rev. D* 98 (3) (2018) 030001, <https://doi.org/10.1103/PhysRevD.98.030001>.
- [17] J. Birrell, C.T. Yang, P. Chen, J. Rafelski, Relic neutrinos: physically consistent treatment of effective number of neutrinos and neutrino mass, *Phys. Rev. D* 89 (2014) 023008, <https://doi.org/10.1103/PhysRevD.89.023008>, arXiv:1212.6943 [astro-ph.CO].
- [18] J. Rafelski, C.T. Yang, The muon abundance in the primordial universe, *Acta Phys. Pol. B* 52 (2021) 277, <https://doi.org/10.5506/APhysPolB.52.277>, arXiv:2103.07812 [hep-ph].
- [19] I. Kuznetsova, J. Rafelski, Unstable hadrons in hot hadron gas in laboratory and in the early universe, *Phys. Rev. C* 82 (2010) 035203, <https://doi.org/10.1103/PhysRevC.82.035203>, arXiv:1002.0375 [hep-th].
- [20] J. Rafelski, C.T. Yang, Reactions governing strangeness abundance in primordial universe, arXiv:2009.05661 [hep-ph], Contribution to SQM2021 Online Conference, May 17–22, 2021.
- [21] J. Cugnon, R.M. Lombard,  $K^+$  production in a cascade model for high-energy nucleus-nucleus collisions, *Nucl. Phys. A* 422 (1984) 635–653, [https://doi.org/10.1016/0375-9474\(84\)90369-5](https://doi.org/10.1016/0375-9474(84)90369-5).
- [22] J. Birrell, J. Rafelski, Quark-gluon plasma as the possible source of cosmological dark radiation, *Phys. Lett. B* 741 (2015) 77, <https://doi.org/10.1016/j.physletb.2014.12.033>, arXiv:1404.6005 [nucl-th].
- [23] A.G. Riess, The expansion of the universe is faster than expected, *Nature Rev. Phys.* 2 (1) (2019) 10–12, <https://doi.org/10.1038/s42254-019-0137-0>, arXiv:2001.03624 [astro-ph.CO].
- [24] L. Verde, T. Treu, A.G. Riess, Tensions between the early and the late universe, *Nat. Astron.* 3 (2019) 891, <https://doi.org/10.1038/s41550-019-0902-0>, arXiv:1907.10625 [astro-ph.CO].
- [25] A.G. Aksenov, R. Ruffini, G.V. Vereshchagin, Thermalization of nonequilibrium electron-positron-photon plasmas, *Phys. Rev. Lett.* 99 (2007) 125003, <https://doi.org/10.1103/PhysRevLett.99.125003>.
- [26] A.G. Aksenov, R. Ruffini, G.V. Vereshchagin, Pair plasma relaxation time scales, *Phys. Rev. E* 81 (2010) 046401, <https://doi.org/10.1103/PhysRevE.81.046401>.